AAC Journals.ASM.org

Mutations in Genes for the F_{420} Biosynthetic Pathway and a Nitroreductase Enzyme Are the Primary Resistance Determinants in Spontaneous *In Vitro*-Selected PA-824-Resistant Mutants of *Mycobacterium tuberculosis*

Hana L. Haver,[a,b] Adeline Chua,[a] Pramila Ghode,[a,c] Suresh B. Lakshminarayana,[a] Amit Singhal,[d] Barun Mathema,[e] René Wintjens,[f] Pablo Bifani[a]

Novartis Institute for Tropical Diseases, Singapore[a]; Department of Microbiology and Immunology Program, Yong Loo Lin School of Medicine, Life Sciences Institute, National University of Singapore, Singapore[b]; Department of Biological Sciences, Faculty of Science, National University of Singapore, Singapore[c]; Singapore Immunology Network (SIgN), A*STAR, Singapore[d]; Department of Epidemiology, Mailman School of Public Health, Columbia University, New York, New York, USA[e]; Laboratory of Biopolymers and Supramolecular Nanomaterials (CP206/04), Université Libre de Bruxelles, Brussels, Belgium[f]

Alleviating the burden of tuberculosis (TB) requires an understanding of the genetic basis that determines the emergence of drug-resistant mutants. PA-824 (pretomanid) is a bicyclic nitroimidazole class compound presently undergoing the phase III STAND clinical trial, despite lacking identifiable genetic markers for drug-specific resistant *Mycobacterium tuberculosis*. In the present study, we aimed to characterize the genetic polymorphisms of spontaneously generated PA-824-resistant mutant strains by surveying drug metabolism genes for potential mutations. Of the 183 independently selected PA-824-resistant *M. tuberculosis* mutants, 83% harbored a single mutation in one of five nonessential genes associated with either PA-824 prodrug activation (*ddn*, 29%; *fgd1*, 7%) or the tangential F_{420} biosynthetic pathway (*fbiA*, 19%; *fbiB*, 2%; *fbiC*, 26%). Crystal structure analysis indicated that identified mutations were specifically located within the protein catalytic domain that would hinder the activity of the enzymes required for prodrug activation. This systematic analysis conducted of genotypes resistant to PA-824 may contribute to future efforts in monitoring clinical strain susceptibility with this new drug therapy.

Tuberculosis (TB) remains a major global health concern, with >8 million new cases and 1.8 million deaths occurring annually (WHO). This pandemic is exacerbated by the pervasive spread of multidrug-resistant (MDR)-TB that challenges clinicians to fight a disease with a limited arsenal of resources. The bicyclic 4-nitroimidazole chemotype has yielded two promising candidates, delamanid (OPC67683) and pretomanid (PA-824), which actively inhibit both nonreplicating and rapidly growing bacilli under aerobic and anaerobic conditions (1). Both drugs are undergoing clinical evaluation and FDA approval is pending for the treatment of MDR-TB. In 2013, delamanid received conditional marketing authorization by the European Medicines Agency (EMA) for use in adult patients deprived of other treatment options (2). PA-824 is in the phase III STAND clinical trial, and at this stage of the development pipeline, it would be beneficial to monitor the genetic basis of resistant clinical strains as they emerge in the wake of future implementation into a treatment protocol.

Bicyclic 4-nitroimidazoles are prodrugs that require metabolic activation by a deazaflavin (cofactor F_{420})-dependent nitroreductase (Ddn) (3). Ddn (Rv3547) converts the prodrugs into three primary metabolites, a des-nitroimidazole and two unstable byproducts (4). Ddn is likely a membrane-bound protein (5) that is involved in a protective mechanism under oxidative stress (6). The major mechanism of action of nitroimidazole in active disease under aerobic conditions is to hinder the formation of mycolic acids, and under anaerobic conditions, the mechanism involves the induction of respiratory poisoning (4, 7). By inhibiting the formation of ketomycolates, a class of mycolic acids, nitroimidazole interferes with *Mycobacterium tuberculosis* cell wall formation, thus curtailing growth (1). PA-824 also donates nitric oxide (NO), which can accumulate and create toxic conditions within the bacilli that hamper regular electron flow and homeostasis during latency (4). In active aerobic *M. tuberculosis*, this NO buildup is insufficient to have a significant bactericidal effect (7).

The two-electron transfer cofactor F_{420} (7,8-didemethyl-8-hydroxy-5-deazaflavin derivative), first reported in mycobacteria (8), plays a role in redox reactions and the methane biosynthesis pathway (9–11). F_{420} redox cycling requires the NADP-dependent glucose-6-phosphate dehydrogenase (FGD1) to catalyze the oxidation of glucose-6-phosphate to 6-phosphogluconolactone. After the reduction of F_{420} to the active protonated cofactor, F_{420}-H_2, Ddn catalyzes the reverse reaction to oxidize it back to F_{420}. It has been hypothesized that Ddn orients PA-824 so that hydride

Received 7 February 2015 **Returned for modification** 28 February 2015
Accepted 9 June 2015

Accepted manuscript posted online 22 June 2015

Citation Haver HL, Chua A, Ghode P, Lakshminarayana SB, Singhal A, Mathema B, Wintjens R, Bifani P. 2015. Mutations in genes for the F_{420} biosynthetic pathway and a nitroreductase enzyme are the primary resistance determinants in spontaneous *in vitro*-selected PA-824-resistant mutants of *Mycobacterium tuberculosis*. Antimicrob Agents Chemother 59:5316–5323. doi:10.1128/AAC.00308-15.

Address correspondence to Pablo Bifani, pablo.bifani@novartis.com.

A.C. and P.G. contributed equally to this article.

Supplemental material for this article may be found at http://dx.doi.org/10.1128/AAC.00308-15.

doi:10.1128/AAC.00308-15

The authors have paid a fee to allow immediate free access to this article.

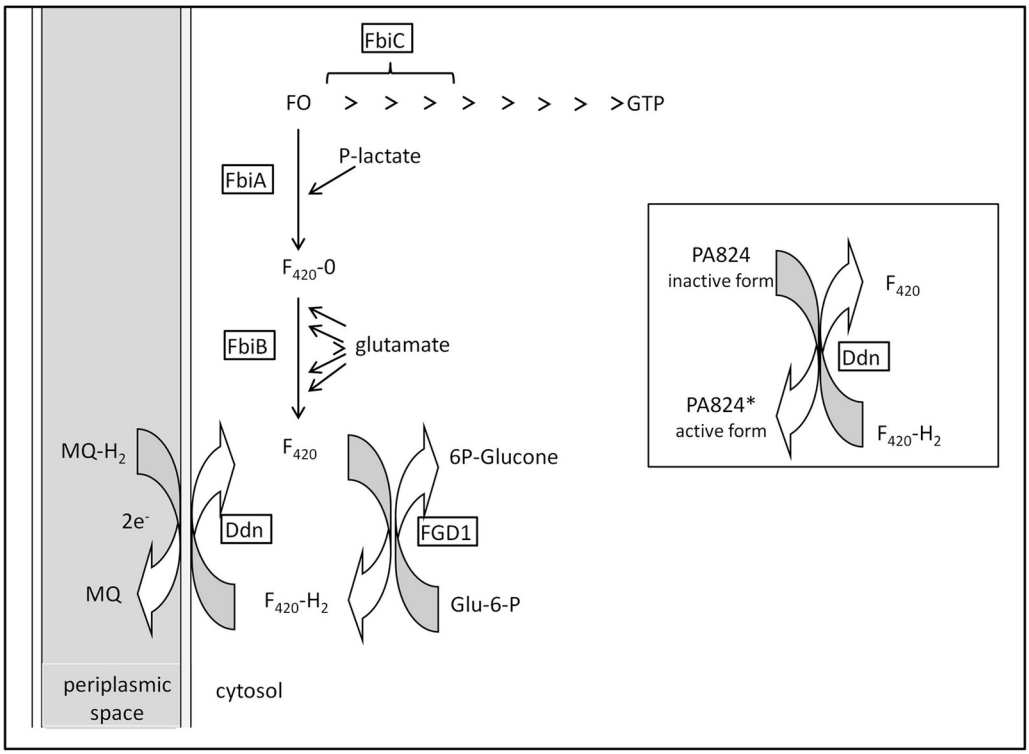

FIG 1 Cofactor F_{420} biosynthetic pathway. 6P-glucone, 6-phosphogluconolactone; Glu-6-P, glucose 6-phosphate; FO, 7,8-didemethyl-8-hydroxy-5-deazariboflavin (a 5-deazaflavin biosynthetic intermediate of F_{420}); F_{420}-0, FO with side chain phospholactyl; F_{420}, F_{420}-0 with *n* glutamate moieties ($n = 5$ or 6); $F_{420}-H_2$, reduced coenzyme F_{420}; P-lactate, 2-phospho-L-lactate; MQ, menaquinone; $MQ-H_2$, menaquinol (reduced menaquinone).

transfer from F_{420} can occur and stabilize the transition state during this biochemical reaction (5). In F_{420} biosynthesis, the FbiC gene encodes a 7,8-didemethyl-8-hydroxy-5-deazariboflavin (FO) synthase, which transfers the hydroxybenzyl group from 4-hydroxy-phenylpyruvate to pyrimidinedione (12). FbiA and FbiB are subsequently involved in the addition of 2-phospho-L-lactate and polymerization of the penta-polyglutamate tail that generates the F_{420} cofactor (13). FbiA is a 2-phospho-L-lactate transferase responsible for the transfer of the lactyl phosphate moiety of lactyl-2-diphospho-5′-guanosine to FO and is known as CofD in *Methanosarcina mazei* (14). The biosynthetic contributions of FbiA, FbiB, and FbiC to PA-824 resistance were determined in studies of transposon mutagenesis mutants (13, 15). A susceptible phenotype could be reintroduced by complementation, confirming that F_{420} depletion is one of the mechanisms of resistance to this compound class (13). The crystal structures and functions of FbiA from *M. mazei* (14) and FbiB from *Archaeoglobus fulgidus* (16) were recently deciphered; the functions are depicted in Fig. 1.

Stover et al. (1) selected spontaneous mutants in the presence of PA-824 and found that those strains could not carry out the nitro-reduction required for drug activation, averting bactericidal consequences. Mutant strains containing mutated FGD1, a critical component of F_{420} activation, conferred PA-824 resistance (1, 13, 15). Choi et al. (13) generated transposon mutants resistant to PA-824, and of those that displayed a negative phenotype for F_{420} production, insertions were identified in either *fbiA* or *fbiB*, for which complementation could restore production. Ddn, FGD1, and FbiA were reported to be nonessential to the optimal growth of *M. tuberculosis in vitro*, and there are no available data on the essentiality of FbiB and FbiC (17). While findings suggest that the mechanisms of resistance to PA-824 are not essential to proliferation when cells are grown *in vitro* under aerobic conditions, it is unclear whether they affect the organism while under oxidative stress. Looking forward toward potential implementation in the clinical setting, it is helpful to note that PA-824 exhibits no cross-resistance (18) with other antitubercular drugs, heightening optimism for its use in TB control of multidrug resistant bacilli.

In this study, we used *M. tuberculosis* strain H37Rv to perform a forward population genetics evaluation of PA-824 resistance. Our aims were to (i) collect spontaneously generated *M. tuberculosis* strains with a PA-824-resistant phenotype under aerobic conditions, (ii) characterize the genotypes of five genes associated with either PA-824 prodrug activation (*ddn* and *fgd*1) or the tangential F_{420} biosynthetic pathway (*fbiA*, *fbiB*, and *fbiC*), (iii) incorporate mutation and frequency findings into drug target binding models for Ddn and FGD1, and (iv) assess the relative degree of bacterial resistance in representative mutant strains.

MATERIALS AND METHODS

Antibiotics, bacterial strains, and selection of spontaneous mutants. PA-824 was synthesized and its purity confirmed as previously described (3). *M. tuberculosis* strain H37Rv (ATCC 29294) was cultured in 7H9 (BD Difco Middlebrook 7H9 broth) liquid medium at 37°C to an optical density at 590 nm (OD_{590}) of 0.6 ($\sim 1 \times 10^8$ CFU) for the selection of mutants on agar plates containing either 1 or 5 μM (0.36 or 1.79 μg/ml, respectively) PA-824 under aerobic conditions. The starting inoculum was determined by serial dilution and plating on agar plates in triplicate. As an additional control, two inocula (10^8 and 10^9) were plated on 1 μg/ml

TABLE 1 Frequency of mutations associated with PA-824 resistance at 1 and 5 μM

PA-824 concn	No. of colonies/plate for:		
	10^5 CFU plated	10^6 CFU plated	10^7 CFU plated
1 μM	3, 2, 2, 1, 0, 0, 0, 0	28, 28, 25, 18, 17, 17, 14, 6	>40[a]
Frequency	1×10^{-5}	1.9×10^{-5}	
5 μM	None	None	16, 8, 7, 5, 4, 4, 4, 3
Frequency			6.38×10^{-7}

[a] Exact number was not recorded.

rifampin yielding 1 to 10 colonies per plate, respectively. After incubation of the seeded plates for 4 weeks at 37°C, resistant colonies were selected and subcultured in 1 ml of 7H9 liquid medium containing an equivalent concentration of the drug used for selection for 12 days. Extracted DNA was used for PCR of the five putative resistance-determining regions, and their corresponding upstream region of 68 to 195 bp were sequenced and analyzed. Sanger sequencing was performed using BigDye Terminator version 3.1 cycle sequencing (1st Base Asia). Five independent selection experiments were performed. All five genes (*ddn*, *fgd1*, *fbiA*, *fbiB*, and *fbiC*) were sequenced for the first selection experiment only, comprising 91 samples. For the four subsequent selection experiments, samples were sequenced sequentially, starting with *ddn*, *fgd1*, *fbiA*, *fbiB*, and *fbiC* until a mutation was identified. For the four subsequent selection experiments, 10^7 and 10^8 bacilli were plated on five plates each at 1 and 5 μM (20 plates per experiment, for 100 plates total), and eight plates for each batch were used to pick three colonies per plate. The primers used for amplification and sequencing are found in Table S1 in the supplemental material.

Determination of MICs. Transparent flat-bottomed 24-well plates (Nunc) were filled with 1 ml of 7H11 agar containing various drug concentrations of PA-824 (0, 0.5, 1.0, 5.0, and 10.0 μM) and prepared based on previously reported MICs and laboratory observations. A 100-μl culture of *M. tuberculosis* at an OD_{590} 0.02 (~1×10^6 CFU) was seeded and incubated at 37°C for 3 to 4 weeks. The MIC_{99} was assigned at the concentration at which no growth was observed.

RESULTS

Frequency of spontaneous mutations in PA-824. Spontaneous PA-824-resistant mutants were selected throughout five independent biological experiments, with each experiment distinctly performed on a different date starting from an independent inoculum. The range in mutation rates was determined to be 10^{-5} to 10^{-7} CFU in the first selection experiment and found to vary according to the concentrations of PA-824. H37Rv cultures were adjusted to 10^5, 10^6, 10^7, 10^8, and 10^9 CFU and plated on 7H11 (BD Difco 7H11) agar plates containing either 1 or 5 μM PA-824 (eight plates each). Only 8 CFU were recovered from the eight plates of 10^5 CFU at 1 μM and none at 5 μM; consequently, the mutation rate was found to be 1×10^{-5} at 1 μM and undetectable at 5 μM for 1×10^5 CFU. CFU were recovered on plates containing 1 μM PA-824 that had been plated with 10^6 CFU and on plates containing 5 μM PA-824 at $\geq 10^7$ CFU. No mutants were selected from plates containing 5 μM PA-824 when plating 10^6 bacilli (Table 1). In the four subsequent selection experiments, only 10^7 and 10^8 CFU were seeded on each plate, from which only three colonies per plate were randomly picked.

Distribution of genetic polymorphisms, structural analysis, and homology modeling. Out of 203 PA-824-resistant *M. tuberculosis* colonies that were selected and subcultured, 20 were eliminated from the study due to either failure of growth or reconfirmation of resistance. Of the 183 isolated strains that were subjected to target sequencing using PCR, lesions in *ddn* were most prevalent, accounting for 29% ($n = 53$), followed by 26% in *fbiC* ($n = 47$), 19% in *fbiA* ($n = 35$), 7% in *fgd1* ($n = 12$) and 2% in *fbiB* ($n = 4$), and the remaining 17% ($n = 32$) harbored no mutations in the five genes examined (Fig. 2). Insertions and deletions accounted for 36 mutant isolates with lesions on *ddn* ($n = 6$), *fgd1* ($n = 3$), *fbiA* ($n = 13$), *fbiB* ($n = 1$), and *fbiC* ($n = 13$), and 40 samples had substitutions leading to an early termination codon *ddn* ($n = 34$), *fgd1* ($n = 2$), *fbiA* ($n = 2$), *fbiB* ($n = 1$), and *fbiC* ($n = 1$) (Fig. 2).

Of the *ddn* mutants, 58% (31/53) had mutations leading to a ^{11}Ser→STOP substitution, resulting in an early stop codon (Table 2). Eighteen other polymorphisms, including 15 distinct mutations were identified, with three clusters comprising three ^{133}Tyr→Asp and two ^{88}Trp→Arg mutations and two insertions of ^{55}Arg. There were three single and one dinucleotide deletions and two insertions of one and seven amino acids. All insertions were in-frame, and all deletions were out-of-frame. The mutation of ^{22}Ser→Leu mirrored previously reported single nucleotide polymorphisms (SNPs). ^{22}Ser→Ala and ^{22}Ser→Val correlated to strong decreased enzymatic activity *in vitro* (6). Modeling analysis based on existing crystal structures was completed for the Ddn protein (PDB code 3R5R) (5) (Fig. 3). The ^{86}Pro→Leu and ^{88}Trp→Arg mutations lost contact with F_{420} and lost a side chain H-bond with F_{420}, respectively (see Fig. S1 in the supplemental material). The two insertions of one and seven amino acids were both found in a loop interacting with the polyglutamate tail of F_{420} (see Fig. S1) (5), and ^{133}Tyr→Asp mutation localizes in the PA-824 putative binding site.

The crystal structure of FGD1 cocrystallized with F_{420} was used to model the mutations encountered in the present study (PDB code 3B4Y) (Table 2 and Fig. 4A) (19). The ^{106}Gly→Val mutation is located within the F_{420}-binding site. The ^{112}Asn→Lys mutation forms an H-bond with F_{420}, and the ^{43}Pro→Arg and ^{230}Glu→Lys

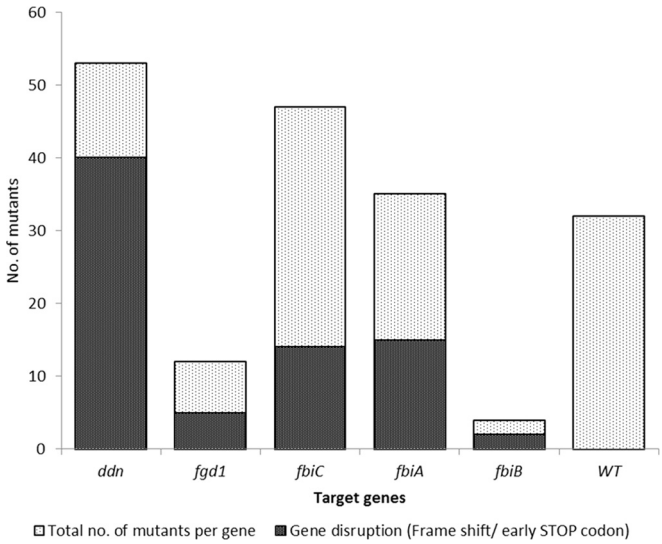

FIG 2 Distribution of mutation frequencies among the five target genes. The relative number of genes encoding early STOP codons and out-of-frame insertions and deletions is shown in gray.

TABLE 2 Summary of mutations identified in genes *ddn* and *fgd1*

nt change by gene	aa change	Frequency	Concn used for selection (μM)	Comment(s)
Gene Rv3547/*ddn*				
$^{24\Delta}$T	^{8}Phe→Phe	1	5	Single-nucleotide deletion→frameshift
^{32}C→A	^{11}Ser→STOP	31	1/5	Early termination codon
^{65}C→T	^{22}Ser→Leu	1	1	Decrease in enzyme activity (5)
$^{72/73\Delta}$TA	^{24}Ile→Ile	1	1	Double-nucleotide deletion→frameshift
$^{73\Delta}$A	25-Asn→Ile	1	1	Single-nucleotide deletion→frameshift
^{87}C →A	^{29}Tyr→STOP	1	5	Early termination codon
^{124}C→T	^{42}Gln→STOP	1	5	Early termination codon
^{143}T→C	^{48}Leu→Pro	1	5	Single-nucleotide substitution
^{163}CGC	^{55}Arg	2	1	In-frame 1-aa insertion; loop interacting with polyglutamate tail of F_{420}
^{163}21 bp	^{55}7 aa	1	5	In-frame 7-aa insertion; loop interacting with polyglutamate tail of F_{420}
^{232}T→C	^{78}Ser→Pro	1	1	Single-nucleotide substitution
^{242}G→A	^{81}Gly→Asp	1	1	Flanking F_{420}-interacting residue
^{257}C→T	^{86}Pro→Leu	1	5	Substitution loses contact with F_{420} cofactor
^{262}T→C	^{88}Trp→Arg	2	1	Loss of H-bond with F_{420}
$^{290\Delta}$A	^{97}Lys→Arg	1	5	Single-nucleotide deletion→frameshift
^{320}T→C	^{107}Leu→Pro	1	1	Partially accessible β-strand flanking F_{420}-binding site
^{361}G→A	^{121}Glu→Lys	1	1	Single-nucleotide substitution
^{397}T→G	^{133}Tyr→Asp	3	5	Localize in PA-824 putative binding site; substitutions of ^{133}Tyr previously shown to abolish activity (5)
^{409}C→T	^{137}Gln→STOP	1	5	Nucleotide substitution→early termination codon
Total no. of *ddn* mutants		53		
Gene Rv0407/*fgd*1				
^{128}C→G	^{43}Pro→Arg	2	5	Putative glucose-6-phosphate-binding site (16)
^{212}G→A	^{71}Gly→Asp	1	1	Flanks F_{420}-binding site
^{317}G→T	^{106}Gly→Val	1	1	Putative F_{420}-binding site
^{336}C→A	^{112}Asn→Lys	1	5	Putative H-bond with F_{420} cofactor
$^{146\Delta}$GCCATG	^{129}Gly→Ala, $^{130\Delta}$H, $^{131\Delta}$A	1	5	Out-of-frame 6-nt (2-aa) deletion
^{428}G→A	^{143}Trp→STOP	1	1	Nucleotide substitution→early termination codon
^{429}G→A	^{143}Trp→STOP	1	5	Nucleotide substitution→early termination codon
$^{498\Delta}$C	^{166}Pro→Pro	1	5	Single-nucleotide deletion→frameshift
^{506}G→C	^{169}Gly→Ala	1	5	Loop distant from active site, function unknown
$^{678\Delta}$A	^{227}Asp→Glu	1	5	Single-nucleotide insertion→frameshift
^{688}G→A	^{230}Glu→Lys	1	1	Putative glucose-6-phosphate-binding site (16)
Total no. of *fgd1* mutants		12		

mutations are predicted to bind the substrate glucose-6-phosphate (19). Two of the mutants led to different SNPs on codon ^{143}Trp, resulting in an early STOP codon. In addition, an out-of-frame six-nucleotide deletion responsible for a two-amino acid deletion (^{130}His and ^{131}Ala) and a mutation (^{129}Gly→Ala) were noted.

Twenty-eight different mutations in 35 independent mutants were identified in *fbiA*, including 13 frameshift mutations and two early stop codons (Fig. 5; see also Table S2 in the supplemental material). The crystal structure of CofD, an ortholog of FbiA from *M. mazei*, has been solved in complex with the FO moiety and GDP (PDB code 3C3E) (14). Sequence similarity between *M. mazei* CofD and *M. tuberculosis* FbiA proteins suggests that the ^{63}Asp→Gly mutation could be involved in binding of the FO molecule, but this is not sufficient to predict the influence of mutation on FbiA function in the remaining 14 strains.

Genetic alterations in *fbi*C accounted for 26% ($n = 47$) of the mutants (Fig. 5; see also Table S2 in the supplemental material). Distinct mutations were observed in 38 isolates, including those leading to one early stop codon and 13 out-of-frame insertions and deletions. The codon leads to the ^{372}Pro→Ser, ^{387}Asp→Tyr, ^{720}Val→Ile mutations, and an insertion of ^{843}C accounted for three, two, four, and four mutants, respectively. Since there is no available crystal structure for FbiC, we could not elucidate a predictable model for PA-824-resistant mutants.

Four mutations within *fbiB* were identified, including a 17-nucleotide insertion and one leading to a stop codon (Fig. 5; see also Table S2 in the supplemental material). The ^{361}Pro→Ala mutation was located within the FbiB C-terminal domain (portion 245 to 448), whose function remains unknown, and the N-terminal domain encompassed the coenzyme F_{420}-0:γ-glutamyl ligase enzyme. Based on comparative analysis with the structure of a homologous enzyme from *A. fulgidus* (16), the ^{153}Gly→Val mutation likely localized within the putative active site of the enzyme. To our knowledge, this is the first data reported on mutations in *fbiA* and *fbiB* associated with PA-824, two genes associated with

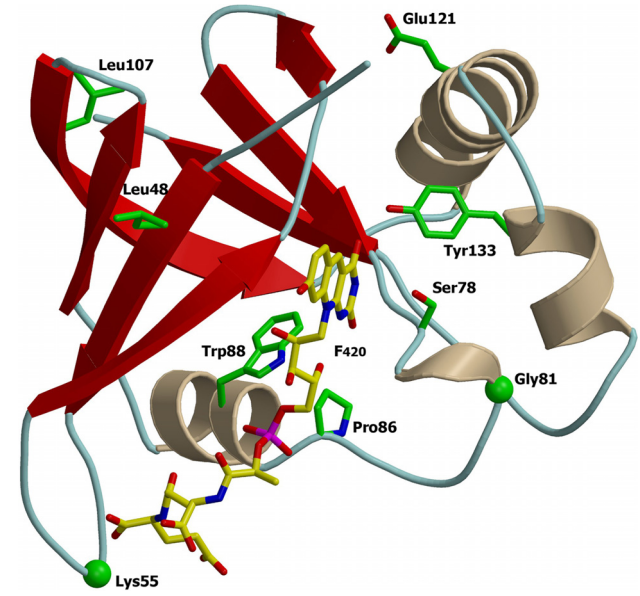

FIG 3 Ribbon representations of *Mycobacterium* protein Ddn (PDB code 3R5R). Mutated residues identified are represented on the three-dimensional (3D) protein structures. The F_{420} is depicted with carbon atoms in yellow. The images were obtained using a consecutive combination of the MolScript (37) and Raster3D (38) programs.

bicyclic nitroimidazole resistance. This finding can likely be attributed to the strategy of sequencing all the genes for 91/183 spontaneous mutants associated with the F_{420} biosynthetic pathway coupled with the large number of isolates analyzed.

The annotated reading frames of *fbiA* and *fbiB* overlap by four nucleotides at the C terminus of *fbiA*. It is possible that the predicted starting codon of *fbiB* is downstream. Alternatively, the start codon and an additional nucleotide of *fbiB* might be part of the last codon of *fbiA* and its termination. This phenomenon is not unusual in plants, whereby two overlapping reading frames can be cotranscribed in a bicistronic mRNA (18).

MIC determination. The MIC_{99} was determined for 40 strains on 7H11 agar containing various concentrations of PA-824 (0, 0.5, 1.0, 5.0, and 10.0 μM). The strains used for MIC_{99} determination were randomly selected prior to knowledge of the sequencing results. Of those mutants exhibiting a high level of resistance, the greatest proportion (56% [$n = 15$]) led to the ^{11}Ser→STOP mutation in *ddn*, a single-nucleotide deletion and frameshift at ^{25}Asn in *ddn*, a single-nucleotide deletion and frameshift at ^{52}Gly in *fbiC*, a ^{86}Tyr→STOP mutation in *fbiC*, and a single-nucleotide deletion and resulting frameshift at ^{71}Gly, ^{74}Asp, and ^{81}Gln in *fbiA*.

DISCUSSION

This study aimed to characterize the genetic polymorphisms of spontaneously generated PA-824-resistant mutant strains by examining drug metabolism genes for potential mutations. The frequency of mutations ranged from 1×10^{-5} to 10^{-7} in a concentration-dependent manner, which was higher than that previously reported (6.7×10^{-7} to 9.0×10^{-7}) (1). Hurdle et al. (20) selected nitrofuranylamide-resistant *M. tuberculosis* mutants and reported a frequency of 10^{-5} to 10^{-7}, which was more consistent with our findings and similar to that for isoniazid (21). Concentration dependency was reflected in the increased number of CFU found on plates containing the lowest drug concentration. Noteworthy is the dose of 50 mg/kg of body weight of PA-824 utilized in *in vivo*

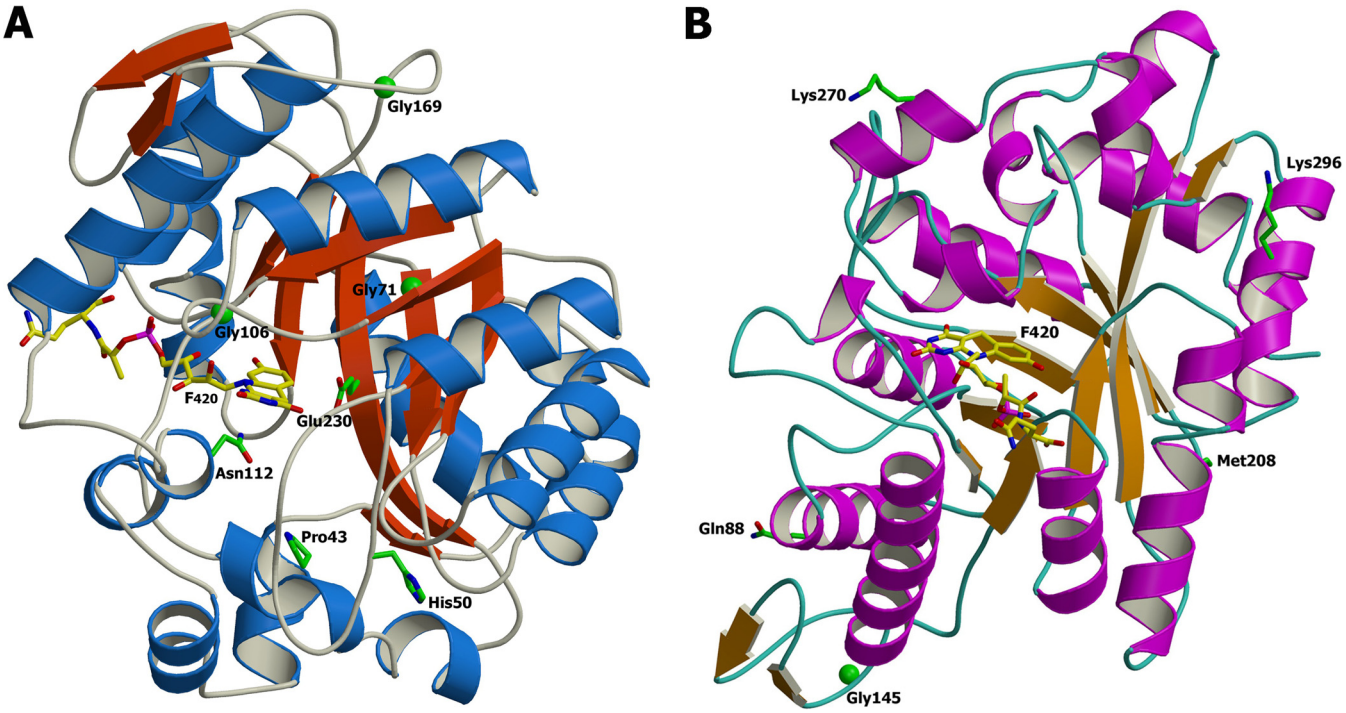

FIG 4 Ribbon representation of the crystal structure of *Mycobacterium* FGD1 (PDB code 3BY4) (A) Mutated residues identified are represented on the 3D protein structures. The F_{420} is depicted with carbon atoms in yellow. Phylogenetic amino acid substitutions reported by Feuerriegel et al. (35) are shown (B). These residues are found on the protein surface. The image was produced consecutively using the MolScript (37) and Raster3D (38) programs.

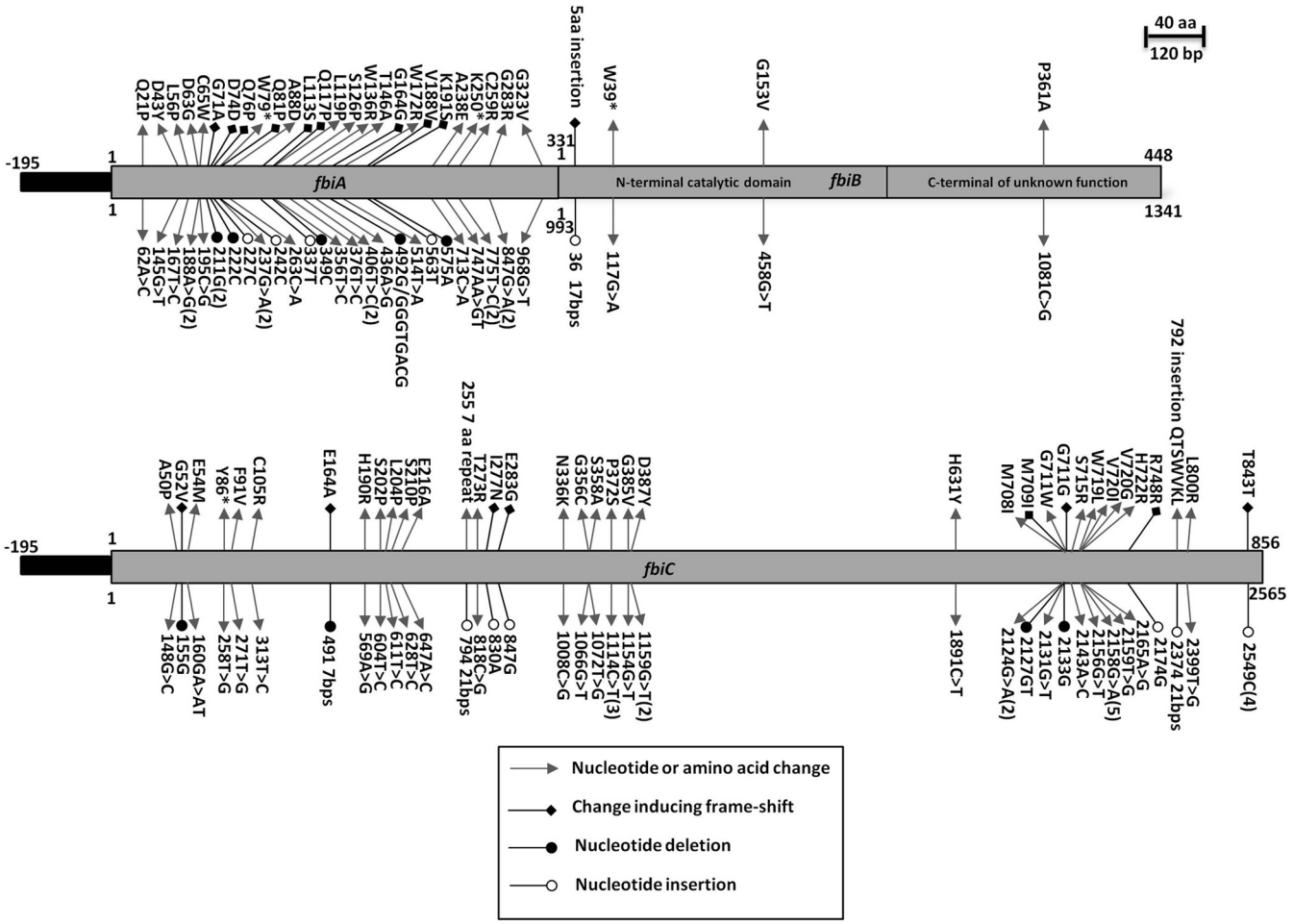

FIG 5 Schematic representation of the mutations found in fbiABC.

combination studies in mouse models, which corresponds to approximately 30 μM, or roughly six times the concentration used to select for mutants in this study (22–25). With the currently recommended 200-mg dose (26) of PA-824 and the corresponding concentration observed *in vivo* in humans (~2 to 3 μM [27]), we predict that the mutation frequency will fluctuate around 10^{-6}, although other environmental factors or host immunity may influence this estimate (28). This prediction underscores the critical need for proper drug combination and dosing to avoid the early emergence of drug resistance. The ongoing STAND phase III clinical trial is evaluating a combination of pyrazinamide, PA-824, and moxifloxacin, of which both pyrazinamide and PA-824 have a high frequency of emergent drug resistance, while moxifloxacin shares extensive cross-resistance with other fluoroquinolones (29, 30).

Adding to previous reports of mutations in the *ddn*, *fgd1*, and *fbiC* genes, we found an association between mutations in *fbiA* and *fbiB* and PA-824 resistance that supports the transposon mutagenesis work of Choi et al. (13, 15). In assessing the genetic polymorphisms in genes associated with PA-824 prodrug activation (*ddn* and *fgd1*) and the tangential F_{420} biosynthetic pathway (*fbiA*, *fbiB*, and *fbiC*), we hoped to gain a better understanding of the genetic underpinnings that determine the emergence of drug resistance. Within these five genes, we found a diverse set of changes in the majority of the PA-824-resistant mutant strains that were incorporated into a predicted crystal structure analysis of Ddn and FGD1. These structures indicate that identified mutations were specifically located within the protein catalytic domain that would hinder the activity of the enzymes required for prodrug activation.

The greatest diversity in SNP insertions and deletions was identified in *fbiC* and *fbiA*. Besides the original transposon mutagenesis reports by Choi et al. (13, 15), no SNPs have been reported in these two genes. The number of early truncations or frameshifts identified in all 5 examined drug target genes corroborate the notion that these enzymes are nonessential for growth under aerobic conditions (17); this finding is similar to those mutations associated with other prodrugs used to treat TB, including ethionamide, pyrazinamide, and *para*-aminosalicylic acid (29). In contrast, Gurumurthy et al. (6) found *fbiC*-deficient *M. tuberculosis* mutants to be hypersensitive to oxidative stress and more susceptible to antitubercular drugs, including isoniazid, moxifloxacin, and clofazimine.

Resistant mutants were organized into three groups: (i) those with complete protein disruption due to a frameshift or early termination, (ii) those with altered critical residues interacting with either the cofactor or substrate, and (iii) those with substitutions for which the function could not be predicted in this study.

Functional redundancy or functional analogs have often been observed in TB, as demonstrated for the 2 isocitrate lyases (31), the 2 thymidylate synthases (32, 33), and the RibD recently identified as a member of the dihydrofolate superfamily (34). The orthologs Rv1261c and Rv1558 may be functional analogs of Ddn (6), while other enzymes (Rv1155 and Rv2991) have been found to be structural analogs of FGD1 (3). In a pool of 65 PA-824-susceptible clinical isolates, Feuerriegel et al. (35) identified five unique phylogenetic or neutral SNPs in *fgd1*. Accordingly, the FGD1 model elucidated in this study shows that these phylogenetic SNPs are dispersed outside the F_{420}-binding site and are not found in the *M. tuberculosis* H37Rv resistant mutants selected here (Fig. 4B). Detrimental mutations on the catalase-peroxidase (KatG) required for the activation of the prodrug isoniazid are extremely rare given the associated significant loss of bacterial fitness. In contrast, changes in pyrazinamidase (PncA) associated with pyrazinamide resistance can include complete disruption of the gene with no known associated fitness cost (29). In this study, no visible fitness cost was observed *in vitro*, as determined aerobically by growth kinetics (data not shown), which is reminiscent of mutants with changes in PncA. It is important to bear in mind that the mutants reported here were identified by analysis of randomly selected mutants aerobically *in vitro* and may not corroborate to the ratio or targets observed clinically, as previously observed in the cases of ethionamide (P. Bifani and A. Chua, unpublished data) and isoniazid (36).

The wide distribution and diversity of mutations might present a challenge for the development of a molecular diagnostic hybridization-based assay test, such as GeneXpert MTB/RIF or GenoType MTBDR*plus*. It is possible that the molecular profile for PA-824 resistance in clinical isolates will prove to be more restrictive due to unforeseen fitness costs in the patient; hence, a molecular diagnostic approach could be reconsidered.

The frequency of mutations in PA-824-resistant *M. tuberculosis* was found to be elevated when selecting at 1 μM and similar to that of isoniazid at 5 μM. Of the resistant strains examined, 83% had single mutations in one of the five genes associated with PA-824 drug metabolism, either directly (*ddn* and *fgd1*) or indirectly (*fbiA*, *fbiB*, and *fbiC*). The remaining 17% of the mutants had no identifiable lesions within these genes, and this suggests that other targets might be involved in either the activation pathway or the mechanism of action of the drug. Correlating mutation types and MIC_{99} is an important next step. The mutant frequency and consequent fitness have yet to be determined in clinical isolates, as nitroimidazoles have not yet been introduced into standard clinical practice. With this systematic analysis of PA-824-resistant *M. tuberculosis* mutants, we aimed to provide a reference to support the tools used to monitor TB drug resistance.

ACKNOWLEDGMENTS

H.L.H. is a fellow of the Joint Master of Science in Infectious Diseases, Vaccinology & Drug Discovery, National University of Singapore (NUS), the Novartis Institute for Tropical Diseases (NITD), the University of Basel (UB), and the Swiss Tropical and Public Health Institute (STPH). R.W. is a research associate at the National Fund for Scientific Research (FNRS-FRS) (Belgium). P.B. is an adjunct staff, Department of Microbiology and Immunology Program, Yong Loo Lin School of Medicine, NUS.

H.L.H., B.M., and P.B. developed the concept; A.C. and P.B. carried-out biosafety level 3 (BSL3) work, including spontaneous-resistant mutant selection; P.G. and H.L.H. sequenced and analyzed the spontaneous mutants; R.W. performed the protein modeling; R.W. H.L.H, A.S., S.B.L., and P.B. analyzed the results; and H.L.H., A.C., B.M., R.W., and P.B. wrote the paper.

REFERENCES

1. **Stover CK, Warrener P, VanDevanter DR, Sherman DR, Arain TM, Langhorne MH, Anderson SW, Towell JA, Yuan Y, McMurray DN, Kreiswirth BN, Barry CE, Baker WR.** 2000. A small-molecule nitroimidazopyran drug candidate for the treatment of tuberculosis. Nature **405:** 962–966. http://dx.doi.org/10.1038/35016103.
2. **European Medicines Agency.** 2013. European Medicines Agency recommends two new treatment options for tuberculosis. EMA/717915/2013. European Medicines Agency, London, United Kingdom. http://www.ema.europa.eu/ema/index.jsp?curl=pages/news_and_events/news/2013/11/news_detail_001972.jsp&mid=WC0b01ac058004d5c1.
3. **Manjunatha UH, Boshoff H, Dowd CS, Zhang L, Albert TJ, Norton JE, Daniels L, Dick T, Pang SS, Barry CE, III.** 2006. Identification of a nitroimidazo-oxazine-specific protein involved in PA-824 resistance in *Mycobacterium tuberculosis*. Proc Natl Acad Sci U S A **103:**431–436. http://dx.doi.org/10.1073/pnas.0508392103.
4. **Singh R, Manjunatha U, Boshoff HI, Ha YH, Niyomrattanakit P, Ledwidge R, Dowd CS, Lee IY, Kim P, Zhang L, Kang S, Keller TH, Jiricek J, Barry CE, III.** 2008. PA-824 kills nonreplicating *Mycobacterium tuberculosis* by intracellular NO release. Science **322:**1392–1395. http://dx.doi.org/10.1126/science.1164571.
5. **Cellitti SE, Shaffer J, Jones DH, Mukherjee T, Gurumurthy M, Bursulaya B, Boshoff HI, Choi I, Nayyar A, Lee YS, Cherian J, Niyomrattanakit P, Dick T, Manjunatha UH, Barry CE, III, Spraggon G, Geierstanger BH.** 2012. Structure of Ddn, the deazaflavin-dependent nitroreductase from *Mycobacterium tuberculosis* involved in bioreductive activation of PA-824. Structure **20:**101–112. http://dx.doi.org/10.1016/j.str.2011.11.001.
6. **Gurumurthy M, Rao M, Mukherjee T, Rao SP, Boshoff HI, Dick T, Barry CE, III, Manjunatha UH.** 2013. A novel F(420)-dependent antioxidant mechanism protects *Mycobacterium tuberculosis* against oxidative stress and bactericidal agents. Mol Microbiol **87:**744–755. http://dx.doi.org/10.1111/mmi.12127.
7. **Manjunatha U, Boshoff HI, Barry CE.** 2009. The mechanism of action of PA-824: novel insights from transcriptional profiling. Commun Integr Biol **2:**215–218. http://dx.doi.org/10.4161/cib.2.3.7926.
8. **Cousins FB.** 1960. The prosthetic group of a chromoprotin from mycobacteria. Biochim Biophys Acta **40:**532–534. http://dx.doi.org/10.1016/0006-3002(60)91396-2.
9. **Jones WJ, Nagle DP, Jr, Whitman WB.** 1987. Methanogens and the diversity of archaebacteria. Microbiol Rev **51:**135–177.
10. **Bleicher K, Winter J.** 1991. Purification and properties of F_{420}- and NADP(+)-dependent alcohol dehydrogenases of *Methanogenium liminatans* and *Methanobacterium palustre*, specific for secondary alcohols. Eur J Biochem **200:**43–51. http://dx.doi.org/10.1111/j.1432-1033.1991.tb21046.x.
11. **Purwantini E, Daniels L.** 1996. Purification of a novel coenzyme F_{420}-dependent glucose-6-phosphate dehydrogenase from *Mycobacterium smegmatis*. J Bacteriol **178:**2861–2866.
12. **Li H, Xu H, Graham DE, White RH.** 2003. Glutathione synthetase homologs encode alpha-L-glutamate ligases for methanogenic coenzyme F_{420} and tetrahydrosarcinapterin biosyntheses. Proc Natl Acad Sci U S A **100:**9785–9790. http://dx.doi.org/10.1073/pnas.1733391100.
13. **Choi KP, Bair TB, Bae YM, Daniels L.** 2001. Use of transposon Tn*5367* mutagenesis and a nitroimidazopyran-based selection system to demonstrate a requirement for *fbiA* and *fbiB* in coenzyme F(420) biosynthesis by *Mycobacterium bovis* BCG. J Bacteriol **183:**7058–7066. http://dx.doi.org/10.1128/JB.183.24.7058-7066.2001.
14. **Forouhar F, Abashidze M, Xu H, Grochowski LL, Seetharaman J, Hussain M, Kuzin A, Chen Y, Zhou W, Xiao R, Acton TB, Montelione GT, Galinier A, White RH, Tong L.** 2008. Molecular insights into the biosynthesis of the F_{420} coenzyme. J Biol Chem **283:**11832–11840. http://dx.doi.org/10.1074/jbc.M710352200.
15. **Choi KP, Kendrick N, Daniels L.** 2002. Demonstration that *fbiC* is required by *Mycobacterium bovis* BCG for coenzyme F(420) and FO biosynthesis. J Bacteriol **184:**2420–2428. http://dx.doi.org/10.1128/JB.184.9.2420-2428.2002.
16. **Nocek B, Evdokimova E, Proudfoot M, Kudritska M, Grochowski LL,**

White RH, Savchenko A, Yakunin AF, Edwards A, Joachimiak A. 2007. Structure of an amide bond forming F(420):gamma-glutamyl ligase from *Archaeoglobus fulgidus*–a member of a new family of non-ribosomal peptide synthases. J Mol Biol **372:**456–469. http://dx.doi.org/10.1016/j.jmb.2007.06.063.

17. **Griffin JE, Gawronski JD, Dejesus MA, Ioerger TR, Akerley BJ, Sassetti CM.** 2011. High-resolution phenotypic profiling defines genes essential for mycobacterial growth and cholesterol catabolism. PLoS Pathog **7:**e1002251. http://dx.doi.org/10.1371/journal.ppat.1002251.
18. **Hiesel R, Brennicke A.** 1985. Overlapping reading frames in *Oenothera mitochondria*. FEBS Lett **193:**164–168. http://dx.doi.org/10.1016/0014-5793(85)80143-5.
19. **Bashiri G, Squire CJ, Moreland NJ, Baker EN.** 2008. Crystal structures of F_{420}-dependent glucose-6-phosphate dehydrogenase FGD1 involved in the activation of the anti-tuberculosis drug candidate PA-824 reveal the basis of coenzyme and substrate binding. J Biol Chem **283:**17531–17541. http://dx.doi.org/10.1074/jbc.M801854200.
20. **Hurdle JG, Lee RB, Budha NR, Carson EI, Qi J, Scherman MS, Cho SH, McNeil MR, Lenaerts AJ, Franzblau SG, Meibohm B, Lee RE.** 2008. A microbiological assessment of novel nitrofuranylamides as anti-tuberculosis agents. J Antimicrob Chemother **62:**1037–1045. http://dx.doi.org/10.1093/jac/dkn307.
21. **Johnson R, Streicher EM, Louw GE, Warren RM, van Helden PD, Victor TC.** 2006. Drug resistance in *Mycobacterium tuberculosis*. Curr Issues Mol Biol **8:**97–111.
22. **Tasneen R, Li SY, Peloquin CA, Taylor D, Williams KN, Andries K, Mdluli KE, Nuermberger EL.** 2011. Sterilizing activity of novel TMC207- and PA-824-containing regimens in a murine model of tuberculosis. Antimicrob Agents Chemother **55:**5485–5492. http://dx.doi.org/10.1128/AAC.05293-11.
23. **Harper J, Skerry C, Davis SL, Tasneen R, Weir M, Kramnik I, Bishai WR, Pomper MG, Nuermberger EL, Jain SK.** 2012. Mouse model of necrotic tuberculosis granulomas develops hypoxic lesions. J Infect Dis **205:**595–602. http://dx.doi.org/10.1093/infdis/jir786.
24. **Williams K, Minkowski A, Amoabeng O, Peloquin CA, Taylor D, Andries K, Wallis RS, Mdluli KE, Nuermberger EL.** 2012. Sterilizing activities of novel combinations lacking first- and second-line drugs in a murine model of tuberculosis. Antimicrob Agents Chemother **56:**3114–3120. http://dx.doi.org/10.1128/AAC.00384-12.
25. **Lakshminarayana SB, Boshoff HI, Cherian J, Ravindran S, Goh A, Jiricek J, Nanjundappa M, Nayyar A, Gurumurthy M, Singh R, Dick T, Blasco F, Barry CE, III, Ho PC, Majunatha UH.** 2014. Pharmacokinetics-pharmacodynamics analysis of bicyclic 4-nitroimidazole analogs in a murine model of tuberculosis. PLoS One **9:**e105222. http://dx.doi.org/10.1371/journal.pone.0105222.
26. **Diacon AH, Dawson R, Hanekom M, Narunsky K, Maritz SJ, Venter A, Donald PR, van Niekerk C, Whitney K, Rouse DJ, Laurenzi MW, Ginsberg AM, Spigelman MK.** 2010. Early bactericidal activity and pharmacokinetics of PA-824 in smear-positive tuberculosis patients. Antimicrob Agents Chemother **54:**3402–3407. http://dx.doi.org/10.1128/AAC.01354-09.
27. **Ginsberg AM, Laurenzi MW, Rouse DJ, Whitney KD, Spigelman MK.** 2009. Safety, tolerability, and pharmacokinetics of PA-824 in healthy subjects. Antimicrob Agents Chemother **53:**3720–3725. http://dx.doi.org/10.1128/AAC.00106-09.
28. **McGrath M, Gey van Pittius NC, van Helden PD, Warren RM, Warner DF.** 2014. Mutation rate and the emergence of drug resistance in *Mycobacterium tuberculosis*. J Antimicrob Chemother **69:**292–302. http://dx.doi.org/10.1093/jac/dkt364.
29. **Stoffels K, Mathys V, Fauville-Dufaux M, Wintjens R, Bifani P.** 2012. Systematic analysis of pyrazinamide-resistant spontaneous mutants and clinical isolates of *Mycobacterium tuberculosis*. Antimicrob Agents Chemother **56:**5186–5193. http://dx.doi.org/10.1128/AAC.05385-11.
30. **Diacon AH, Dawson R, von Groote-Bidlingmaier F, Symons G, Venter A, Donald PR, van Niekerk C, Everitt D, Winter H, Becker P, Mendel CM, Spigelman MK.** 2012. 14-day bactericidal activity of PA-824, bedaquiline, pyrazinamide, and moxifloxacin combinations: a randomised trial. Lancet **380:**986–993. http://dx.doi.org/10.1016/S0140-6736(12)61080-0.
31. **Muñoz-Elias EJ, McKinney JD.** 2005. *Mycobacterium tuberculosis* isocitrate lyases 1 and 2 are jointly required for *in vivo* growth and virulence. Nat Med **11:**638–644. http://dx.doi.org/10.1038/nm1252.
32. **Mathys V, Wintjens R, Lefevre P, Bertout J, Singhal A, Kiass M, Kurepina N, Wang XM, Mathema B, Baulard A, Kreiswirth BN, Bifani P.** 2009. Molecular genetics of *para*-aminosalicylic acid resistance in clinical isolates and spontaneous mutants of *Mycobacterium tuberculosis*. Antimicrob Agents Chemother **53:**2100–2109. http://dx.doi.org/10.1128/AAC.01197-08.
33. **Sampathkumar P, Turley S, Ulmer JE, Rhie HG, Sibley CH, Hol WG.** 2005. Structure of the *Mycobacterium tuberculosis* flavin dependent thymidylate synthase (MtbThyX) at 2.0Å resolution. J Mol Biol **352:**1091–1104. http://dx.doi.org/10.1016/j.jmb.2005.07.071.
34. **Zheng J, Rubin EJ, Bifani P, Mathys V, Lim V, Au M, Jang J, Nam J, Dick T, Walker JR, Pethe K, Camacho LR.** 2013. *para*-Aminosalicylic acid is a prodrug targeting dihydrofolate reductase in *Mycobacterium tuberculosis*. J Biol Chem **288:**23447–23456. http://dx.doi.org/10.1074/jbc.M113.475798.
35. **Feuerriegel S, Köser CU, Baù D, Rüsch-Gerdes S, Summers DK, Archer JA, Marti-Renom MA, Niemann S.** 2011. Impact of *Fgd1* and *ddn* diversity in *Mycobacterium tuberculosis* complex on *in vitro* susceptibility to PA-824. Antimicrob Agents Chemother **55:**5718–5722. http://dx.doi.org/10.1128/AAC.05500-11.
36. **Bergval IL, Schuitema AR, Klatser PR, Anthony RM.** 2009. Resistant mutants of *Mycobacterium tuberculosis* selected *in vitro* do not reflect the *in vivo* mechanism of isoniazid resistance. J Antimicrob Chemother **64:**515–523. http://dx.doi.org/10.1093/jac/dkp237.
37. **Esnouf RM.** 1999. Further additions to MolScript version 1.4, including reading and contouring of electron-density maps. Acta Crystallogr D Biol Crystallogr **55:**938–940. http://dx.doi.org/10.1107/S0907444998017363.
38. **Merritt EA, Murphy ME.** 1994. Raster3D version 2.0. A program for photorealistic molecular graphics. Acta Crystallogr D Biol Crystallogr **50:**869–873.